
Supporting Information: Realtime monitoring of polarization state deviations with dielectric metasurfaces

Shaun Lung^a, Jihua Zhang^{a,*}, Kai Wang^b, and Andrey A. Sukhorukov^a

^a*Centre of Excellence for Transformative Meta-Optical Systems (TMOS),*

Department of Electronic Materials Engineering,

Research School of Physics,

The Australian National University,

Canberra, ACT 2601, Australia

^b*Ginzton Laboratory and Department of Electrical Engineering,*

Stanford University, Stanford,

California 94305, United States

**jhzhanghust@gmail.com*

This Supporting Information contains 5 sections and 3 figures, which provide extra details on the theoretical and experimental aspects of our work.

CONTENTS

S1. Optimal symmetrical and non-amplifying transformation	S-2
S2. Experimental characterization methodology	S-3
S3. Determination of the anchor state from the characterized transfer matrix	S-5
S4. Determination of the experimental responsivity parameters from the measured power ratios	S-6
S5. Effect of small deviations in metasurface parameters	S-7

S1. OPTIMAL SYMMETRICAL AND NON-AMPLIFYING TRANSFORMATION

For a given anchor polarization state $|\psi\rangle = [\cos \beta, \sin \beta e^{i\varphi}]^T$ and a target responsivity $\eta_0 = |\alpha|^2$, the necessary transformation will be

$$\mathbf{T} = \xi [|V\rangle \langle \psi| + \gamma |V\rangle \langle \psi_\perp| + \sqrt{\eta_0} |H\rangle \langle \psi_\perp|], \quad (\text{S1})$$

where $|\psi_\perp\rangle = [-\sin \beta e^{-i\varphi}, \cos \beta]^T$ is the orthogonal state of anchor state. Expanding \mathbf{T} , we get

$$\mathbf{T} = \xi \begin{bmatrix} -\sqrt{\eta_0} \sin \beta e^{i\varphi} & \sqrt{\eta_0} \cos \beta \\ \cos \beta - \gamma \sin \beta e^{i\varphi} & \sin \beta e^{-i\varphi} + \gamma \cos \beta \end{bmatrix} \quad (\text{S2})$$

To be a symmetrical matrix, the off-diagonal terms should be equal. This requires that

$$\gamma = -\cot \beta e^{-i\varphi} (\sqrt{\eta_0} - 1), \quad (\text{S3})$$

and it results in

$$\mathbf{T} = \xi \begin{bmatrix} -\sqrt{\eta_0} \sin \beta e^{i\varphi} & \sqrt{\eta_0} \cos \beta \\ \sqrt{\eta_0} \cos \beta & \frac{1 - \sqrt{\eta_0} \cos^2 \beta}{\sin \beta} e^{-i\varphi} \end{bmatrix}. \quad (\text{S4})$$

Another requirement to the transformation is that it does not amplify the input for any polarization. This requires that the maximum singular value of the matrix is no more than one. To realize the optimal transformation with minimum loss, we design the matrix whose maximum singular value is exactly one. Following this, we determine that the optimal symmetrical matrix is the following:

$$\mathbf{T} = \frac{1}{\sigma_{\max}} \begin{bmatrix} -\sin \beta e^{i\varphi} & \cos \beta \\ \cos \beta & \frac{1/\sqrt{\eta_0} - \cos^2 \beta}{\sin \beta} e^{-i\varphi} \end{bmatrix} \quad (\text{S5})$$

where σ_{\max} is the maximum singular value of the matrix

$$\begin{bmatrix} -\sin \beta e^{i\varphi} & \cos \beta \\ \cos \beta & \frac{1/\sqrt{\eta_0} - \cos^2 \beta}{\sin \beta} e^{-i\varphi} \end{bmatrix}. \quad (\text{S6})$$

When the input state is $|\psi\rangle$, the output state after the transformation \mathbf{T} is

$$\mathbf{T}|\psi\rangle = \left[0, \frac{1}{\sigma_{\max} \sqrt{\eta_0}} \right]^T = \xi |V\rangle \quad (\text{S7})$$

Accordingly, we obtain $\xi = 1/(\sigma_{\max} \sqrt{\eta_0})$.

When the input state is $|\psi_{in}\rangle = |\psi\rangle + \delta|\psi_{\perp}\rangle$, the output state is

$$|\psi_{out}\rangle = \mathbf{T}|\psi_{in}\rangle = \xi \begin{bmatrix} \delta\sqrt{\eta_0} \\ 1 - \delta \cot \beta e^{-i\varphi} (\sqrt{\eta_0} - 1) \end{bmatrix} = \xi [|V\rangle + \gamma\delta|V\rangle + \alpha\delta|H\rangle] \quad (\text{S8})$$

Note that, alternately we can also map the anchor state to the horizontal linear polarization based on the same optical setup. In this case, we derive the following optimal symmetrical matrix by using a similar procedure,

$$\mathbf{T} = \frac{1}{\sigma_{\max}} \begin{bmatrix} (1/\sqrt{\eta_0} - \sin^2 \beta) e^{i\varphi} / \cos \beta & \sin \beta \\ \sin \beta & -\cos \beta e^{-i\varphi} \end{bmatrix} \quad (\text{S9})$$

Accordingly, $\gamma = \tan \beta e^{-i\varphi} (\sqrt{\eta_0} - 1)$.

The above results indicate that the value of $|\gamma|$ is fixed for a certain anchor state and target responsivity if we apply a symmetrical transformation. It is better to map the anchor state to the $|H\rangle$ and $|V\rangle$ when β is in the range $0 \sim \pi/4$ and $\pi/4 \sim \pi/2$, respectively, in order to reduce $|\gamma|$. Therefore, the theoretical minimum value of $|\gamma|$ for a symmetrical transformation is

$$|\gamma_{\text{sym}}| = \min \{ \tan \beta, \cot \beta \} (\sqrt{\eta_0} - 1) \quad (\text{S10})$$

Figure S1 shows this theoretical limit of $|\gamma_{\text{sym}}|$ as a function of β and the target responsivity. It also means that $|\gamma_{\text{sym}}|$ is always nonzero when the target responsivity $\eta_0 > 1$ and $|\psi\rangle \neq |H\rangle, |V\rangle$.

S2. EXPERIMENTAL CHARACTERIZATION METHODOLOGY

Due to the design goals of detecting ultrasmall polarization changes, it was necessary to implement a number of measures to resolve practical implementation problems. The measurement system, including the metasurface itself, is by definition highly sensitive to such small polarization

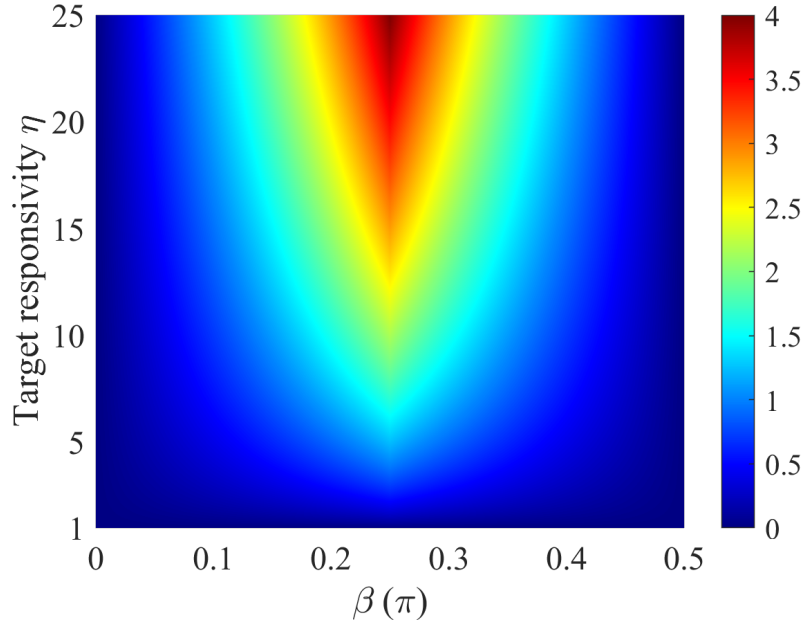


Figure S1. Theoretical limit of $|\gamma_{\text{sym}}|$ as a function of the β of the anchor state and the target responsivity when the transformation matrix is symmetrical (i.e. non-chiral).

changes, including those that might arise from systemic or random error, and thus these had to be accounted for.

We accounted for systemic error arising from non-ideal waveplates by accounting for manufacturer-provided phase retardances. Due to the half- and quarter- waveplates being ideal only at the manufacturer wavelengths of 1550 nm, they would have phase retardances varying away from the correct $\pi/2$ and $\pi/4$ respectively. These errors were corrected for by utilizing the wavelength-retardance relationship as provided by the manufacturer (example shown in Fig. S2) for numerical calculations and fitting of the results. It was also found to be necessary to attain accurate vertical alignment on the order of 0.001° in waveplate alignment by utilizing fixed point calibration via mounted beamsplitter cubes and high-precision servo motors.

During the characterization and experimental process, it was also found to be necessary to judiciously control the incident location and diameter of the beam on the metasurface. This was achieved by utilizing a tightly-focused input beam, however, tight focusing of a polarized beam is known to cause non-uniformity in the polarization^{39,40}, thus resulting in a necessary experimental trade-off in terms of beam polarization and metasurface uniformity. Leaving aside conventional concerns such as requiring a normally incident beam, we observed empirically that the metasur-

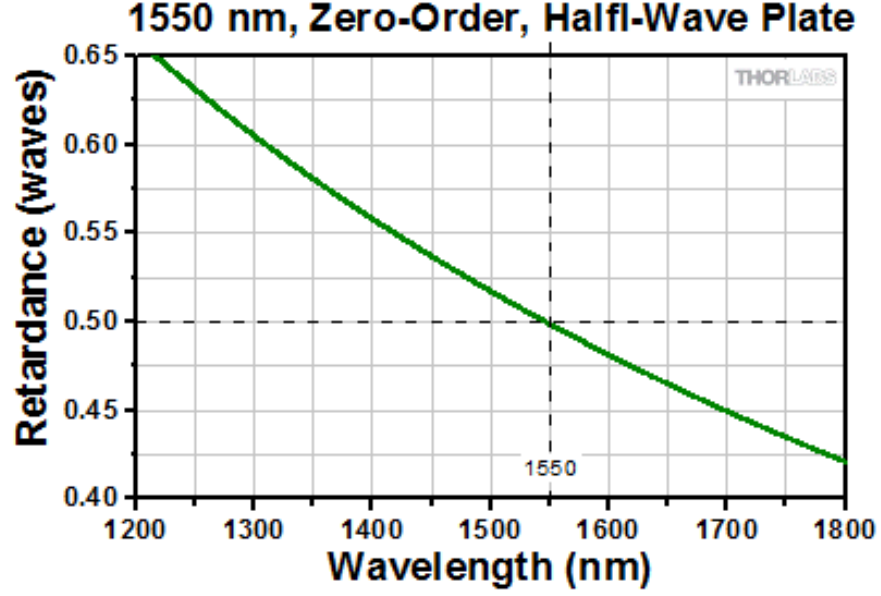


Figure S2. Manufacturer-provided wavelength-retardance relation of the half waveplate utilized in the experimental setup³⁸.

face demonstrated undesirable angular and spatially dependent optical responses, arising from the size and uniformity of the fabrication process. These arose from the non-uniform nanopillar dimensions across the metasurface, which was in turn caused by uncorrected proximity effect during the electron beam lithography. Ultimately, it was determined through empirical means that the beam diameter of approximately $40\mu m$ was an acceptable tradeoff, utilizing a lens of focal length $50mm$. This provided a well-defined polarization while not impinging overly on the fabrication variation across the metasurface.

S3. DETERMINATION OF THE ANCHOR STATE FROM THE CHARACTERIZED TRANSFER MATRIX

After characterizing the transfer matrix to be \mathbf{T} , we calculate the anchor state,

$$|\psi\rangle = \frac{\mathbf{T}^{-1}|\mathbf{V}\rangle}{\|\mathbf{T}^{-1}|\mathbf{V}\rangle\|} \quad (\text{S11})$$

uncertainty factor

$$|\gamma| = \frac{|\langle \mathbf{V} | \mathbf{T} | \psi_{\perp} \rangle|}{|\langle \mathbf{V} | \mathbf{T} | \psi \rangle|} \quad (\text{S12})$$

and responsivity

$$\eta = |\alpha|^2 = \frac{|\langle \mathbf{H} | \mathbf{T} | \psi_{\perp} \rangle|^2}{|\langle \mathbf{V} | \mathbf{T} | \psi \rangle|^2} \quad (\text{S13})$$

These are the equations we have used to obtain the results in Fig. 3 of the main paper.

S4. DETERMINATION OF THE EXPERIMENTAL RESPONSIVITY PARAMETERS FROM THE MEASURED POWER RATIOS

In the measurement, we record the output powers $P_{H,V}$ at different derivations δ near the anchor state. Assuming $|\psi_{in}\rangle = |\psi\rangle + \delta|\psi_{\perp}\rangle$ and $\mathbf{T} = \xi [|\mathbf{V}\rangle\langle\psi| + \gamma|\mathbf{V}\rangle\langle\psi_{\perp}| + \alpha|\mathbf{H}\rangle\langle\psi_{\perp}|]$, we have

$$\frac{P_H}{P_V} = \frac{|\langle \mathbf{H} | \mathbf{T} | \psi_{in} \rangle|^2}{|\langle \mathbf{V} | \mathbf{T} | \psi_{in} \rangle|^2} = \frac{|\alpha\delta|^2}{|1 + \gamma\delta|^2}. \quad (\text{S14})$$

Given that δ is a complex value, any given value of P_H/P_V can, in general, relate to a small spread of values of $|\delta|$ with different phases. This results in a degree of imprecision for any given measurement that is determined by practical concerns, as the proposed measurement scheme cannot yield the complex phase of δ , only allowing for the measurement of $|\delta|$ instead. The maximum and minimum values of $|\delta|$ will be

$$\frac{P_H}{P_V} = \frac{|\alpha|^2 |\delta|_{\max}^2}{(1 + |\gamma| |\delta|_{\max})^2} = \frac{|\alpha|^2 |\delta|_{\min}^2}{(1 - |\gamma| |\delta|_{\min})^2}. \quad (\text{S15})$$

Therefore,

$$|\delta|_{\max} = \frac{\sqrt{P_H/P_V}}{|\alpha| - |\gamma| \sqrt{P_H/P_V}} \approx \sqrt{\frac{P_H/P_V}{\eta}} \left(1 + |\gamma| \sqrt{\frac{P_H/P_V}{\eta}} \right), \quad (\text{S16})$$

$$|\delta|_{\min} = \frac{\sqrt{P_H/P_V}}{|\alpha| + |\gamma| \sqrt{P_H/P_V}} \approx \sqrt{\frac{P_H/P_V}{\eta}} \left(1 - |\gamma| \sqrt{\frac{P_H/P_V}{\eta}} \right). \quad (\text{S17})$$

This means that in the practical case with a nonzero $|\gamma|$, after measuring a specific power ratio the polarization deviation can be determined in a range

$$|\delta| \in \left(\sqrt{\frac{P_H/P_V}{\eta}} - |\gamma| \frac{P_H/P_V}{\eta}, \sqrt{\frac{P_H/P_V}{\eta}} + |\gamma| \frac{P_H/P_V}{\eta} \right). \quad (\text{S18})$$

Accordingly, the uncertainty of measuring $|\delta|$ is

$$\Delta |\delta| = |\delta|_{\max} - |\delta|_{\min} = \frac{2 |\gamma| P_H/P_V}{|\alpha|^2 - |\gamma|^2 P_H/P_V} = 2 |\gamma| |\delta|_{\max} |\delta|_{\min} \approx 2 |\gamma| \frac{P_H/P_V}{\eta}. \quad (\text{S19})$$

For a specific value of P_H/P_V , we can calculate $|\gamma|$ by

$$|\gamma| = \frac{|\delta|_{\max} - |\delta|_{\min}}{2|\delta|_{\max}|\delta|_{\min}}. \quad (\text{S20})$$

Based on this equation, we obtain the experimental $|\gamma|$ using the power measurement at different derivations. The final $|\gamma|$ is taken as the average of the derived $|\gamma|$ obtained at several values of P_H/P_V .

For a specific value of $|\delta|$, the maximum and minimum values of P_H/P_V will be $|\alpha\delta|^2(1 - |\gamma\delta|)^{-2}$ and $|\alpha\delta|^2(1 + |\gamma\delta|)^{-2}$, respectively. Accordingly, the maximum and minimum values of $\sqrt{P_V/P_H}$ are $(1 + |\gamma\delta|)/|\alpha\delta|$ and $(1 - |\gamma\delta|)/|\alpha\delta|$, respectively, if $|\gamma\delta| < 1$. Therefore, we obtain

$$\max\left(\sqrt{P_V/P_H}\right) - \min\left(\sqrt{P_V/P_H}\right) = \frac{2|\gamma\delta|}{|\alpha\delta|} = \frac{2|\gamma|}{|\alpha|}. \quad (\text{S21})$$

Then, we can calculate $|\alpha|$ by

$$|\alpha| = \frac{2|\gamma|}{\max\left(\sqrt{P_V/P_H}\right) - \min\left(\sqrt{P_V/P_H}\right)}. \quad (\text{S22})$$

The experimental responsivity is $\eta = |\alpha|^2$. This allows us to determine the experimental responsivity from the measured power ratios at different deviations. The final η is taken as the average of the derived η obtained at several values of $|\delta|$.

S5. EFFECT OF SMALL DEVIATIONS IN METASURFACE PARAMETERS

To determine the robustness of the metasurface performance under small deviations in its physical dimensions from the numerically optimized values, which might arise from fabrication errors, we performed numerical simulations. We considered the optimized metasurface design corresponding to Figs. 3 and 4 of the main manuscript, and quantified the changes in the metasurface Jones matrix against such variations, see the first two columns in Fig. S3. We observe that there are no sharp changes in the metasurface Jones matrix elements as the physical dimensions are varied. Accordingly, with these changes in dimensions, the chiral response is also preserved, and the anchor state [Fig. S3, third column] also changes slightly. This happens because by design, our metasurface response at the operating wavelength does not feature high-Q optical resonances.

We note that by the definition of responsivity, as in Eq. (S13), high responsivity values imply small values of the denominator. Therefore, small changes in the Jones matrix can have significant effect on the denominator and accordingly the responsivity magnitude, as seen in Fig. S3, fourth

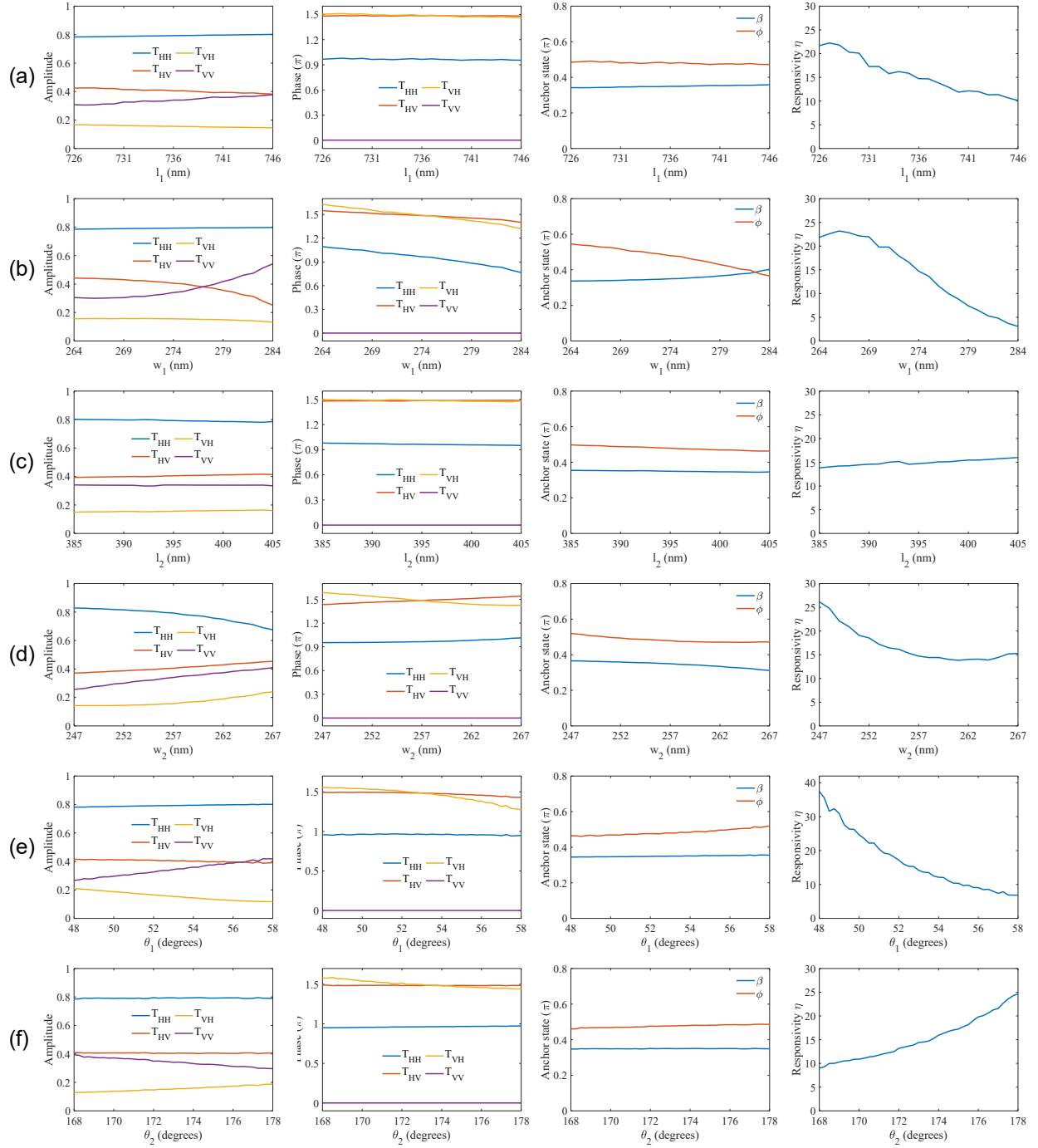


Figure S3. Simulated effects of deviations from the optimized parameters of the metasurface design considered in Figs. 3 and 4 of the main manuscript: (a) l_1 , (b) w_1 , (c) l_2 , (d) w_2 , (e) θ_1 , (f) θ_2 . Here the notations correspond to Fig. 2(a). Shown are the absolute values (first column) and phases (second column) of the Jones matrix elements, the anchor state parameters (third column), and the responsivity (fourth column). These simulations were performed at a wavelength of $1573.8nm$.

column. This confirms that in order to achieve larger responsivity, one requires accordingly higher metasurface fabrication accuracy.